

Large aspect ratio titanate nanowire prepared by monodispersed titania submicron sphere via simple wet-chemical reactions

Baoxiang Wang*, Yong Shi, Dongfeng Xue

State Key Laboratory of Fine Chemicals, Department of Materials Science and Chemical Engineering, School of Chemical Engineering, Dalian University of Technology, 158 Zhongshan Road, Dalian 116012, People's Republic of China

Received 28 October 2006; received in revised form 14 December 2006; accepted 24 December 2006
Available online 17 January 2007

Abstract

A facile one-step hydrothermal reaction among monodispersed titania submicron spheres and KOH solution was found to result in potassium titanate nanowires with a large aspect ratio. The diameter of these nanowires falls in the range of 50–200 nm and the length ranges from several micrometers to several tens of micrometers. It is found that the reaction temperature, duration, titanium source and the size distribution of titania raw powders have a great impact on the resultant morphology. Monodispersed TiO₂ submicron sphere is beneficial for the formation and growth of large-area lamellar potassium titanate and consequently it is in favor of the production of nanowires with a large aspect ratio. The nanowires were analyzed by a range of methods including powder X-ray diffraction (XRD), scanning electron microscope (SEM), high-resolution transmission electron microscopy (HRTEM), selected area electron diffraction (SAED), energy-dispersive X-ray spectrometer (EDX) and UV/Vis spectrophotometer. UV-absorption study showed that these nanowires are wide-band semiconductors with a band gap 3.4 eV. A formation mechanism is proposed on the basis of the dissolving, growth, thickening and splitting of K₂Ti₆O₁₃ nanointermediates.

© 2007 Elsevier Inc. All rights reserved.

Keywords: Nanowire; Hydrothermal; Monodisperse sphere; Nanorod

1. Introduction

One-dimensional TiO₂-related materials with high morphological specificity, such as nanotubes, nanowires, nanosheets, nanoribbons and nanofibers have attracted particular interest because of their unique microstructure and promising functions [1–4]. There is also great interest in the development because of their demonstrated potential in solar energy conversion, photocatalysis, photovoltaic devices, electrochromic devices, antifogging, self-cleaning devices, selective adsorption, ion exchange, ultraviolet blockers and smart surface coatings [5]. Moreover, these nanostructures have the potential to exhibit unusual properties and offers an opportunity to investigate physical and chemical processes in size-confined systems [6–8]. The dimensional confinement and the particular morphology of nanostructure endow them with different and often

enhanced properties mentioned above. There is interest in decreasing the particle size and increasing the surface-to-volume ratio of anatase particles. Thus, TiO₂ nanorods or nanofibers might be exploited in solar cells or photocatalysis where surface-charge recombination is a problem. Titania nanostructures have been produced by a variety of methods including deposition into a nanoporous alumina template, sol-gel transcription using organo-gelators as templates, seeded growth and hydrothermal processes. Although high-temperature reactions, chemical vapor deposition and thermal evaporation have proved to be efficient for the preparation of wire-like nanomaterials, soft-chemical routes are of special focus, with much interest on the preparation of nanostructures of metastable oxide materials [9,10]. For instance, hydrothermal methods have been successfully used to synthesize nanotubes of TiO₂-related materials without using any templates [11–13]. Titania nanotubes with a diameter less than 10 nm could be synthesized by a reaction of NaOH and TiO₂ nanoparticles with anatase or rutile structure, and the obtained

*Corresponding author.

E-mail address: bxwang@dlut.edu.cn (B. Wang).

nanotubes are built in a layered titanate structure trititanate of composition $M_2Ti_3O_7$ or $M_xH_{2-x}Ti_3O_7$ ($M = Na$ or K) [14,15]. Normally raw TiO_2 nanoparticles, such as a commercial anatase powder P25 (Degussa Co., Germany, a mixture of anatase and rutile; its size is less than 30 nm), are usually used as the raw powder reacted with NaOH or KOH [16–18]. The relationship between the size or size distribution of raw TiO_2 powder and the product morphology of hydrothermal reaction is seldom studied. The titanium source may play an important influence on the product of hydrothermal treatment. The exact mechanism of hydrothermal titanate nanowire formation is still a controversial topic debated extensively in contemporary literature.

In this report, we present detailed scanning electron microscopy (SEM) studies on the morphology and structure of titanate nanowires and intermediate products from hydrothermal treatment of monodispersed or polydispersed titania submicron sphere in KOH aqueous solution. The impacts of reaction temperature, duration and titanium source on the morphology of products were clarified. It is observed that not only the reaction temperature, titanium source and duration but also the size and size distribution of titania raw powder have a great impact on the resultant morphology. The results confirm that the structures of resultant nanowires are related to monoclinic layered titanate $K_2Ti_6O_{13}$ or $H_2Ti_6O_{13}$. A formation mechanism is proposed on the basis of the dissolving, growth, thickening and splitting of $K_2Ti_6O_{13}$ nanointermediates.

2. Experimental

2.1. Synthesis of monodispersed titania (anatase) particle by controlled hydrolysis

All chemicals were used as received. Monodispersed spherical TiO_2 particles were prepared by controlled hydrolysis of tetrabutyl titanate (TBT, $Ti(OC_4H_9)_4$, 97%, Aldrich) in ethanol [19]. Typically, 100 mL of ethanol was mixed with 0.4 mL of 0.1 M aqueous potassium chloride, followed by the addition of 2.2 mL of TBT at ambient temperature. The solution was mixed completely using a magnetic stirrer for about 10 min until a white precipitate appeared. The suspension was aged in a static condition for 24 h in a closed container at room temperature in air atmosphere. The powder deposited at the bottom of the vessel was collected and dried at 50 °C in air. Calcinations of amorphous TiO_2 gel at 550 °C gave single-crystalline anatase. Either of the above gel or crystalline anatase monodispersed particles are used as the raw material for the hydrothermal treatment, respectively.

2.2. Synthesis of titanate nanowires by hydrothermal synthesis

In a typical synthesis, titanate nanowires were synthesized by adding monodispersed titania (anatase) particle to

a 10 M aqueous solution of KOH. A total of 0.2 g of monodispersed titania particles and 20 mL of 10 M KOH aqueous solution was mixed and, after stirring for 1 h, the resulting suspension was transferred to a Teflon-lined stainless autoclave. The autoclave was heated and stirred at 180 °C for 10–72 h. After it was cooled down to room temperature, the product was repeatedly and ultrasonically washed by distilled H_2O or a dilute HCl solution (0.1 M) and dried at 80 °C for 6 h.

2.3. Characterization

The microstructure of the samples was observed with a scanning electron microscope (SEM, JSM-5600LV, JEOL, Tokyo, Japan) equipped with an energy-dispersive X-ray (EDX) spectrometer. Transmission electron microscopy (TEM) experiments were performed using a Philips Tecnai G^2 20 microscope operating at 200 kV. The samples were prepared by depositing a drop of the suspension onto a holey carbon grid. The phase composition and crystallinity of the synthesized powders described above were characterized using X-ray powder diffraction (XRD, D/Max 2400, Rigaku Corp., Tokyo, Japan; equipped with graphite monochromatized $CuK\alpha$ radiation) in the 2θ angle ranging from 4° to 80°. The UV/Vis diffuse reflectance spectra were obtained using a UV–Vis–NIR spectrophotometer (JASCO, V-570) using powder samples.

3. Results and discussion

Fig. 1 shows the SEM images of monodispersed and polydispersed TiO_2 particles. Titania particles with narrow size distribution were obtained by controlled hydrolysis starting from tetrabutyl titanate and water in an ethanol solution. Depending on the reaction conditions, particles in the range between 600 and 700 nm were obtained. After calcination, the sizes of these spheres remained unchanged. In contrast, polydispersed TiO_2 particles were also obtained via rapid hydrolysis and its size is ranges from about 100 nm to as large as several micrometers.

Fig. 2 shows the samples prepared by hydrothermal treatment of polydispersed TiO_2 particles at 180 °C for 24 h (a–b) and 72 h (c–d), respectively. Uneven titanate nanorods with low aspect ratio were observed. From the SEM images, the diameter and length of nanorods were about 100–500 nm and several micrometers, respectively. Furthermore, a lot of irregular particles were also found in the product even after 72 h hydrothermal treatment, and this indicates that polydispersed TiO_2 raw powder can impact the important influence on the product.

As can be seen clearly from these SEM images of the hydrothermal reaction products, the potassium titanate (K-titanate) nanowires of a high purity with large aspect ratio were obtained only after reactions at 180 °C for 24 h (As shown in Fig. 3). Monodispersed titania submicron spheres have been transformed into non-hollow nanowires with a small size distribution both in length and in

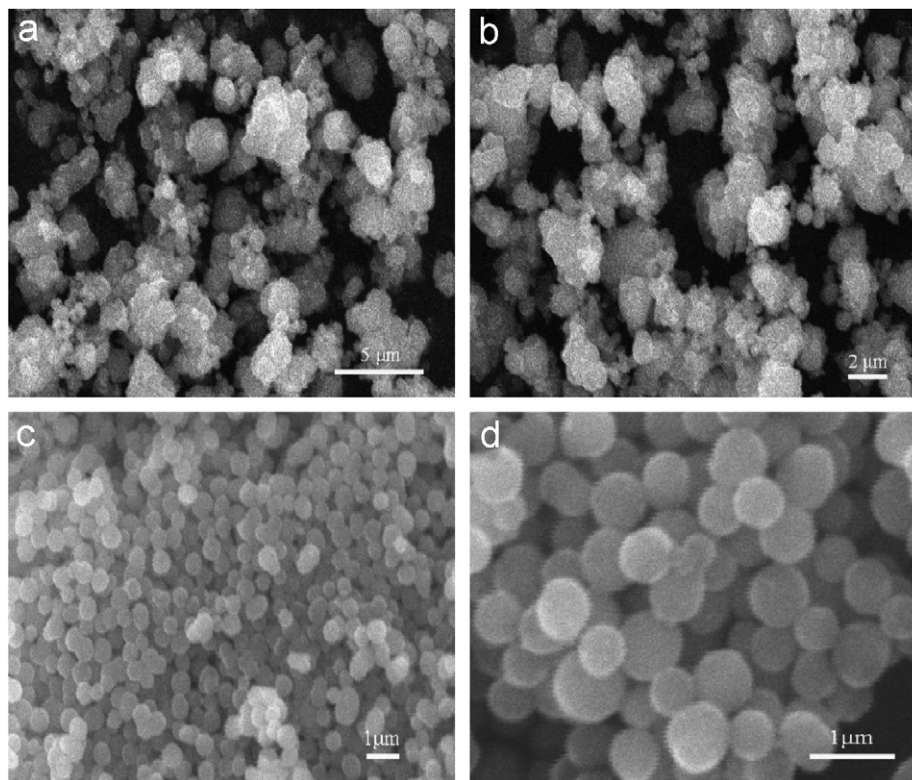


Fig. 1. Raw titania particles: (a, b) polydispersed particle by rapid hydrolysis and (c, d) monodispersed submicron sphere by control hydrolysis.

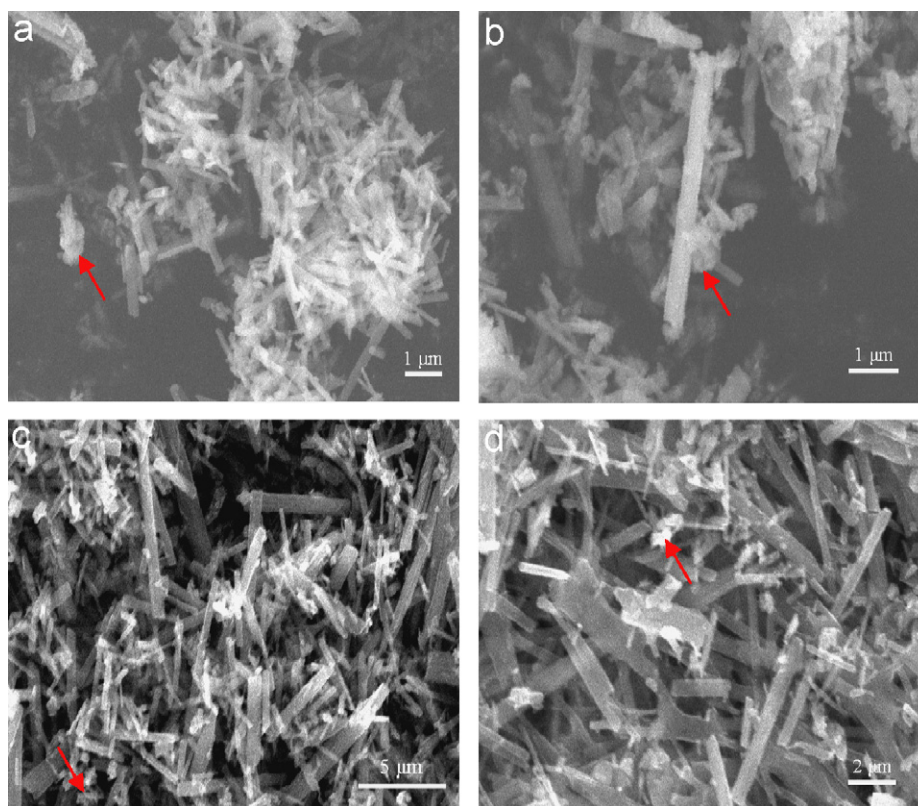


Fig. 2. Nanorod observed for the polydispersed titania sphere after reaction at 180 °C with 10 M KOH: (a, b) 24 h and (c, d) 72 h. (Red arrows indicate the non-rodlike titanate particles.)

diameter. Approximately, the lengths are between several micrometers to several tens of micrometers and the diameters are in the range of 200–300 nm. These products are very different from those nanorods obtained by the hydrothermal treatment of polydispersed titania particles. This also illustrates that the raw materials affect the morphology of the reaction products.

The hydrothermal temperature (T_h) and the concentration of KOH were observed to have a strong effect on the morphological features of the resulting product [20,21]. SEM measurements also show that a hydrothermal treatment of the monodispersed titania submicron sphere at 120 or 150 °C for 24 h (10 M KOH) followed by an ultrasonic dispersion in 0.1 M HCl does not result in the formation of nanostructures. Furthermore, even at 180 °C when the concentration of KOH is low, such as 2 and 5 M, the hydrothermal treatment of similar titania submicron sphere for 24 h does not result in the formation of nanostructures. All these are attributed to the submicron size of raw titania particles. Large raw titania submicron sphere is difficult to dissolve at a low concentration of KOH aqueous solution or at a low hydrothermal temperature.

Therefore, it is interesting to find the brush- or broom-like nanowires that also appeared on the hydrothermal treatment of monodispersed titania sphere treated with 10 M KOH after 24 h at 180 °C. This result is very helpful to understand the formation of nanowires clearly. It is generally recognized that during the treatment with concentrated KOH, some Ti–O bonds of the TiO₂ precursor are broken, leading to the formation of lamellar fragments that are the intermediate phase in the formation process of the nanostructure material. However, why the nanowires formed from the lamellar titanate fragments is unclear. Peng et al. found that the surfaces of the anatase TiO₂ particles were initially smooth. After reacting with KOH aqueous solution for 1 day, many protuberances were formed on the surface of the anatase particle. Furthermore, the structure of the protuberance is the same as that of the nanowires. The nanowires grew out directly from the anatase TiO₂ particles [22]. Yuan et al. revealed

that when the raw material of anatase reacted with KOH solution, some of Ti–O–Ti bonds of titania crystals are broken, and layered octatitanates are formed on the titania surface along the (010) lattice plans of TiO₂. Further, hydrothermal reaction causes the nanowires to grow out along the [010] direction, and nanowires grew out directly from the titania particles [23]. In this report, we can see that the split layer of titanate is indeed the intrinsic reason for the formation of nanowires. From the SEM images (Fig. 4), red arrows indicate the non-split layer titanate, and blue arrows indicate the splitted layer titanate. It is noteworthy that the size and size distribution of the splitted layer titanate is similar to the above-described individual nanowires (see Fig. 3). When the lamellar titanate fragments are formed after the reaction of anatase TiO₂ particles with KOH, these lamellar structures grow and adhere along the [001] direction to form the long lamellar titanate fragments with a large area. Under high temperature and pressure of hydrothermal treatment, these long lamellar titanate fragments begin to split and nanowires with long length are formed.

Extending the hydrothermal time, abundant thin and curved nanowires appeared after reactions 48 and 72 h at 180 °C. Due to the long thick titanate, nanowires begin to further split and the thin nanowires with long length are formed (See Fig. 5). The average nanowire diameter at different reaction times is shown in Table 1. It can be seen that by extending the hydrothermal time, the average diameter is decreased subsequently. Furthermore, thick nanowires are straight due to their rigidity (see Fig. 3), but thin nanowires are flexible and are found to be curved (see Fig. 5d). Similar phenomena were also observed by Wu et al. [12] Approximately for the as-obtained nanowires, the lengths are between several micrometers to several tens of micrometers, and the diameters are in the range of 50–300 nm. Furthermore, the product of the hydrothermal reaction, after neutralizing with 0.1 M HCl solution, is hydrogen titanate (H-titanate) nanowires of the same morphologies as shown in Figs. 3 or 5. Large-area EDX spectra analysis reveals the existence of Ti, K and O in the sample after H₂O washing (Fig. 5e). After HCl/H₂O

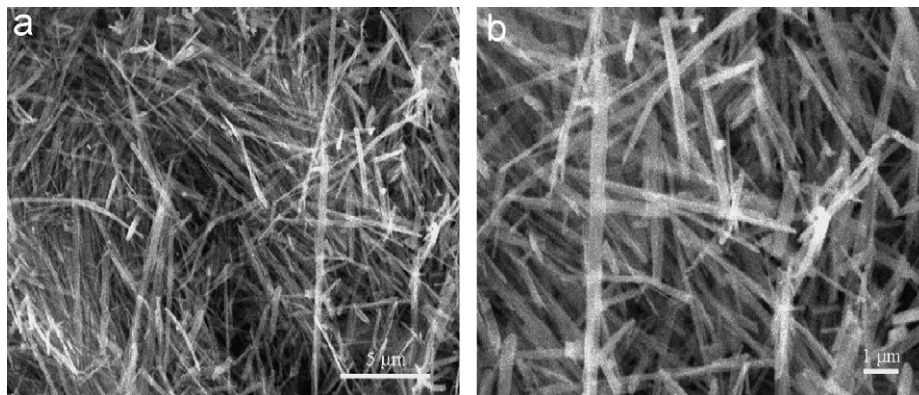


Fig. 3. Low- (a) and (b) high-magnification SEM images of nanowires prepared by the monodispersed titania submicron sphere through hydrothermal treatment; abundant nanowires appeared after reactions 24 h at 180 °C.

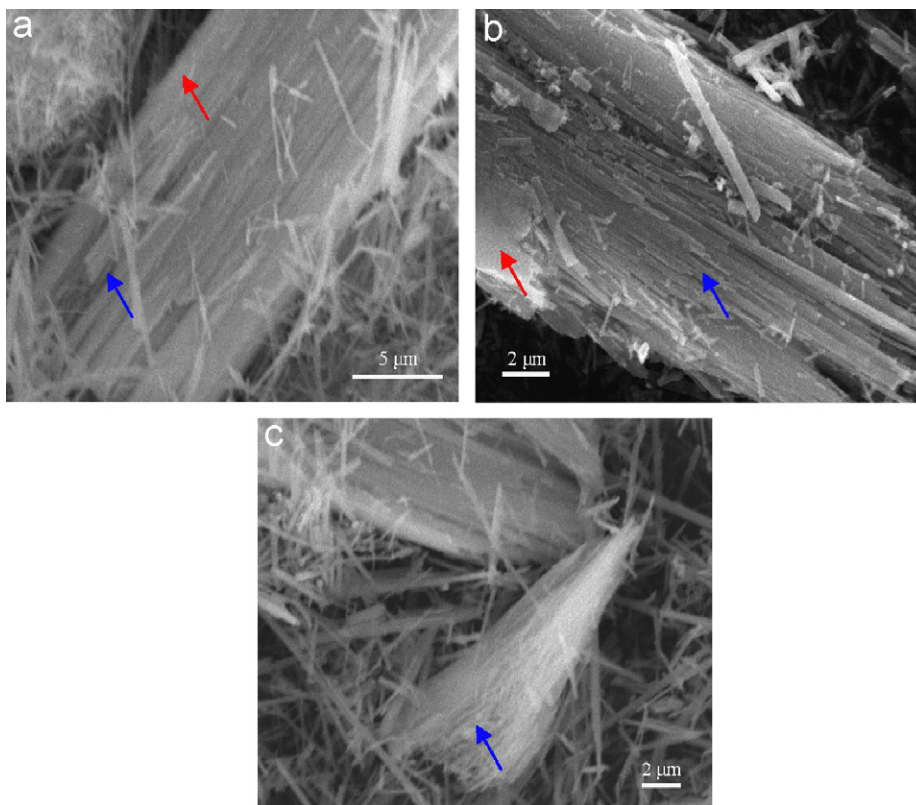


Fig. 4. Brush- or broom-like nanowires obtained by the monodispersed titania sphere treating with 10 M KOH for 24 h at 180 °C. (Red arrows indicate the non-splitted layer titanate; blue arrows indicate the splitted layer titanate.)

washing treatments, only Ti and O are found in the hydrothermal product (Fig. 5f). Neutralization with the dilute acid solution (the pH of the suspension in this step was 7 or above) yielded hydrogen titanate (H-titanate) nanowires that retained the fibril morphology.

The monodispersed titania gel can also be used as the raw material for hydrothermal treatment. Morphology evolution sequence of hydrothermal treatment with different concentrated KOH solution was employed. After 72 h of the monodisperse titania gel treatment with 10 M KOH at 180 °C, a large amount of thin lamellar structures appeared (Fig. 6(a) and (b)), whereas nanorod or nanowire was not found. These thin lamellar structures of potassium titanate are irregular and large than the monodispersed titania gel sphere. Furthermore, its size and thickness indicate that when the lamellar titanate fragments are formed after the reaction of gel particles with KOH, these lamellar structures grow and adhere along the [001] and [010] direction to form the long lamellar titanate fragments with large area. Fig. 6(c) and (d) show the morphology of products for the monodisperse titania gel treated with 15 M KOH at 180 °C for 72 h, Lamellar structures and nanorod products appeared simultaneously; EDX analysis reveals the existence of C, Ti, K and O in the sample, which indicate the existence of organic residue of monodisperse titania gel (Fig. 6e). In order to get the 1D nanostructure product with a high yield, the hydrothermal time or the concentration of KOH must increase for the monodisperse

titanate gel compared with the monodisperse titania anatase particle.

XRD patterns of calcinated monodispersed titania sphere show a typical anatase phase as show in Fig. 7 insert. The changes in the crystal structure from the monodispersed anatase powder to the one-dimensional titanate structure are produced by hydrothermal treatment. The powder XRD pattern of the obtained potassium titanate nanowires is shown in Fig. 7, which can be indexed as a single phase of $K_2Ti_6O_{13}$ (monoclinic phase, space group $C2/m(12)$, JCPDS no. 40-0403, $a = 15.593 \text{ \AA}$, $b = 3.796 \text{ \AA}$, $c = 9.108 \text{ \AA}$ and $\beta = 99.78^\circ$). The broadening of the diffraction peaks indicates the small size of the nanocrystals. The diffraction peak became sharper as the time in the synthesis increased. Furthermore, the XRD pattern of nanowires is similar to that of nanorods obtained by the hydrothermal treatment of polydispersed particles.

Low-magnification TEM image of $K_2Ti_6O_{13}$ nanowires is shown in Fig. 8(a). Fig. 8b shows HRTEM image of nanowires, which also confirms a well-defined single-crystal structure. One set of distinctive lattice fringes parallel to the nanowire axis is observed. The fringe spacing is about 0.78 nm, which corresponds well to the reported interplanar distance for (200) plane of $K_2Ti_6O_{13}$. The growth direction of these titanate nanowires is along the [010] crystal direction. The selected area electron diffraction (SAED) patterns (Fig. 8c) indicate the degree of

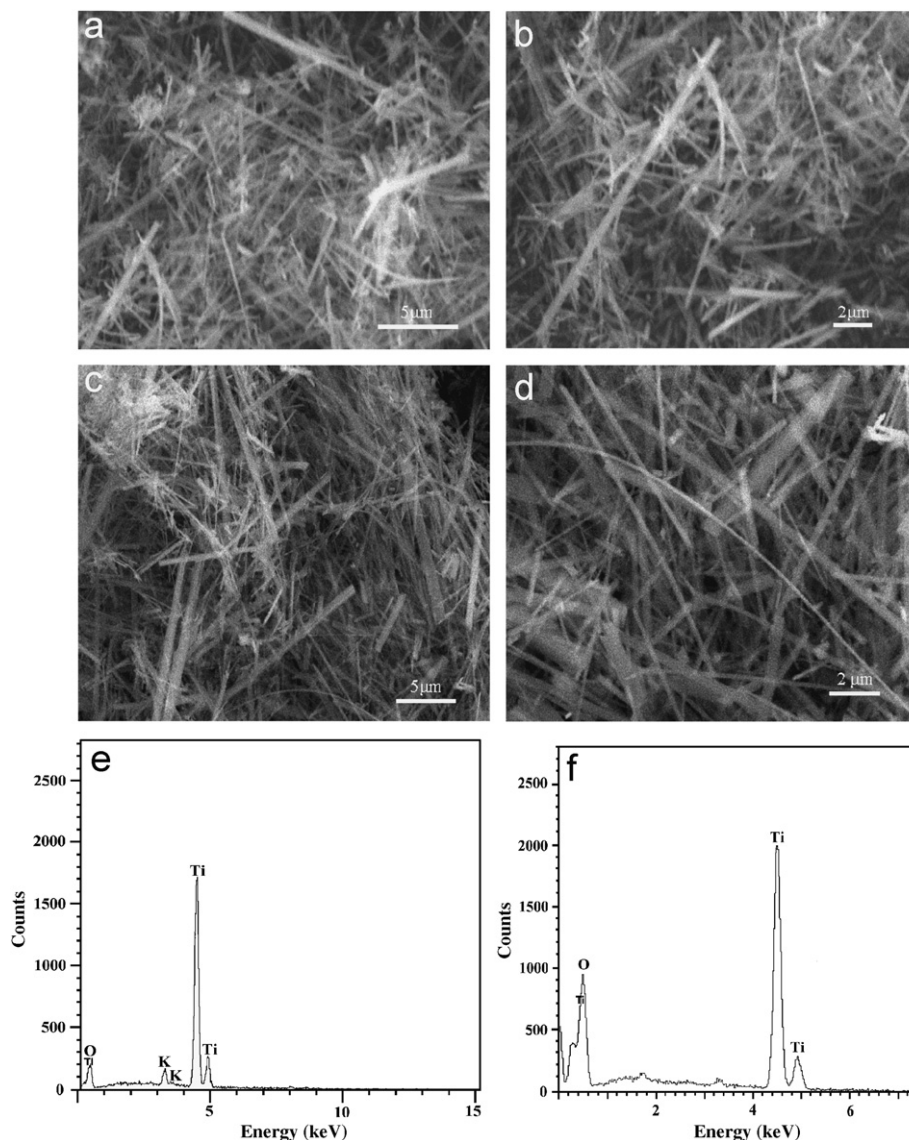


Fig. 5. Potassium titanate or hydrogen titanate nanowire prepared by the monodispersed titania submicron sphere through hydrothermal treatment, and abundant nanowires with large aspect ratio (>200 – 300) appeared after reactions at $180\text{ }^{\circ}\text{C}$ for 48 h (a, b) and 72 h (c, d), respectively. Large-area energy-dispersive X-ray spectra of the potassium titanate and hydrogen titanate nanowires: (e) sample after H_2O washing and (f) sample after $\text{HCl}/\text{H}_2\text{O}$ washing treatments.

Table 1
The average nanowire diameter at different reaction times

Time (h)	24	48	72
Average diameter (nm)	261 ± 40	165 ± 55	78 ± 30

crystallinity and the crystallographic structure of the hydrothermal products. The superlattice reflections from the nanowires indicate that they occur as single crystals.

The crystalline structure of the crystalline TiO_2 polymorphs (such as anatase and rutile) is described with representative Ti-O_6 octahedra which share vertex edges to build up the three-dimensional framework of the oxide. It can be proposed that some of the Ti-O-Ti bonds of the

raw materials are broken when reacted with alkaline solution, and layered titanates composed of octahedral TiO_6 units with the complication of alkali metal ions are formed in the form of thin small sheets. It is noted that the titanate and anatase have common structural features: both crystal lattices consist of the octahedral sharing four edges and the zigzag ribbons. When the crystallographic structure is considered, the titanate has been suggested to comprise of two-dimensional layers, in which TiO_6 octahedral are combined through edge sharing, as shown in Fig. 8(d). It has been reported that adjacent anatase crystallites would coalesce in a way called “oriented attachment” on the high-energy 001 planes, thus leading to the formation of anatase crystals elongating along [001]. This is consistent with the fact that titanate structures have TiO_6 -octahedra as the basic structural units, such that each

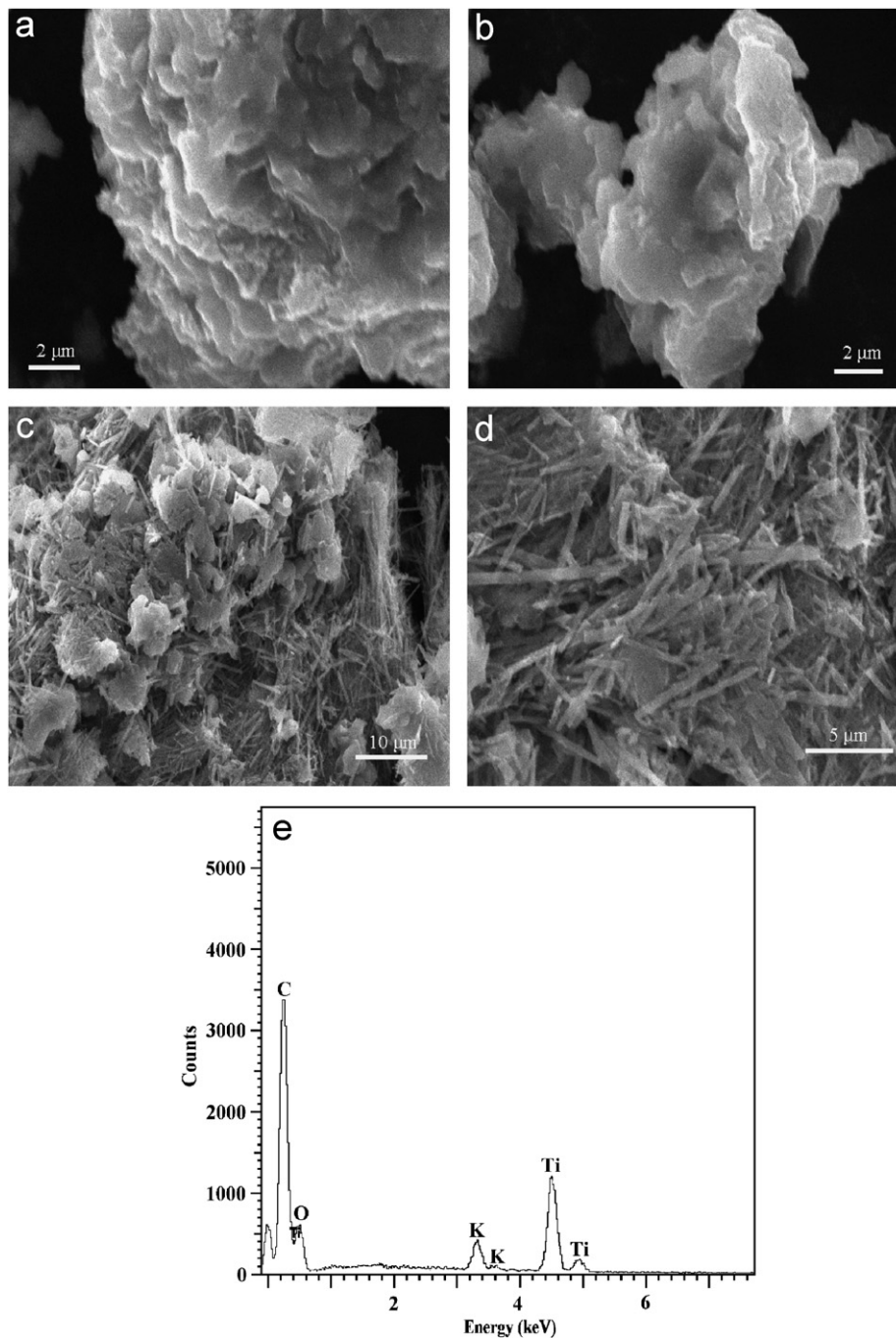


Fig. 6. (a, b) Morphology of products for the monodisperse titania gel treated with 10M KOH at 180 °C for 72 h. Although a large amount of thin lamellar structures appeared, nanorod or nanowire was not found; (c, d) morphology of products for the monodispersed titania gel treated with 15M KOH at 180 °C for 72 h, lamellar structures and nanorod products appeared simultaneously; (e) energy-dispersive X-ray spectra of the above products indicate the existence of organic residue of monodisperse titania gel through the hydrothermal treatment.

TiO₆ octahedron shares edges with other octahedral so as to form a zigzag chain-like structure (see Fig. 8d–g). These chains join together by sharing edges to form layers, and K⁺ ions or protons exist between the layers. So these lamellar structures grow and adhere along the [001] and [010] direction to form long lamellar titanate fragments with large area. For the layered titanate sheets to split, Peng et al. found that surface tension due to an asymmetry related to K or H deficiency in the surface layers of the

plates is the principal driving force of the cleavage [3b]. In order to understand the mechanism of split, except for the structural models of K₂Ti₆O₁₃ shown in Fig. 8(d), the [010] direction, [001] direction and unit cell for the layer K₂Ti₆O₁₃ are provided in Fig. 8. In a layered compound, the chemical bonding between neighboring layers is generally weaker than chemical bonding in the same layers [3,12]. Therefore, the chemical interaction between (100) planes of layer K₂Ti₆O₁₃ is very weak. The intrinsic reason

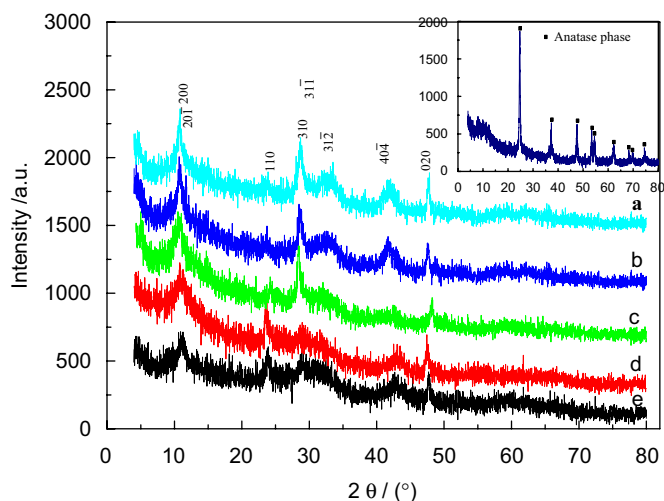


Fig. 7. X-ray diffraction (XRD) patterns of the samples. From the bottom: trace (a–c) XRD patterns of as-prepared titanate nanowires by the hydrothermal treatment for the anatase monodispersed titania particles for 72, 48, 24 h, respectively. Trace (d–e) XRD patterns of as-prepared titanate nanorods by the hydrothermal treatment for the anatase polydispersed titania particles for 72 and 24 h, respectively. Inserts are XRD patterns of the anatase monodispersed titania particles, which indicate a typical anatase phase.

for this is that the strength of K–O bonding is weaker than that of Ti–O bonding of TiO_6 octahedron. Under autoclaving, the high temperature and pressure provide the energy base for the breaking of K–O bonding. So the preferred crystal direction for the splitting should be between (100) and (010) planes due to the easy breaking of K–O bonding. It was observed that nanowires were formed by the splitting of layered crystalline sheets between (100) and (010) planes, as evidenced in Fig. 4. Fig. 4 shows that a bundle of nanowires splitting from the same root is a piece of crystalline sheet. Further splitting of these thick nanowires between (100) and (010) planes can form the thinner nanowires (see Fig. 5).

UV–Vis absorption measurements were also carried out to understand the physical property of the nanowires. Fig. 9 shows three typical UV–Vis absorption spectra obtained from potassium titanate nanowires (trace a synthesized by the monodispersed titania sphere at 180°C for 72 h) and nanorods (trace b synthesized by the polydispersed titania particles at 180°C for 72 h), and anatase monodispersed titania sphere samples. From this figure it is clear that the absorption properties of $\text{K}_2\text{Ti}_6\text{O}_{13}$ nanowires altered significantly. A blue shift is found for the nanowire samples compared with that of nanorod and monodispersed titania sphere; the onset wavelength λ_{onset} of the spectrum recorded from the $\text{K}_2\text{Ti}_6\text{O}_{13}$ nanowire sample is about 370 nm corresponding to a band gap value of 3.40 eV [23]. This value is smaller than the onset wavelength of monodispersed TiO_2 particles with the anatase phase, which is about 400 nm corresponding to a band gap of 3.2 eV. The absorption intensity of the spectrum obtained from the nanostructure sample is

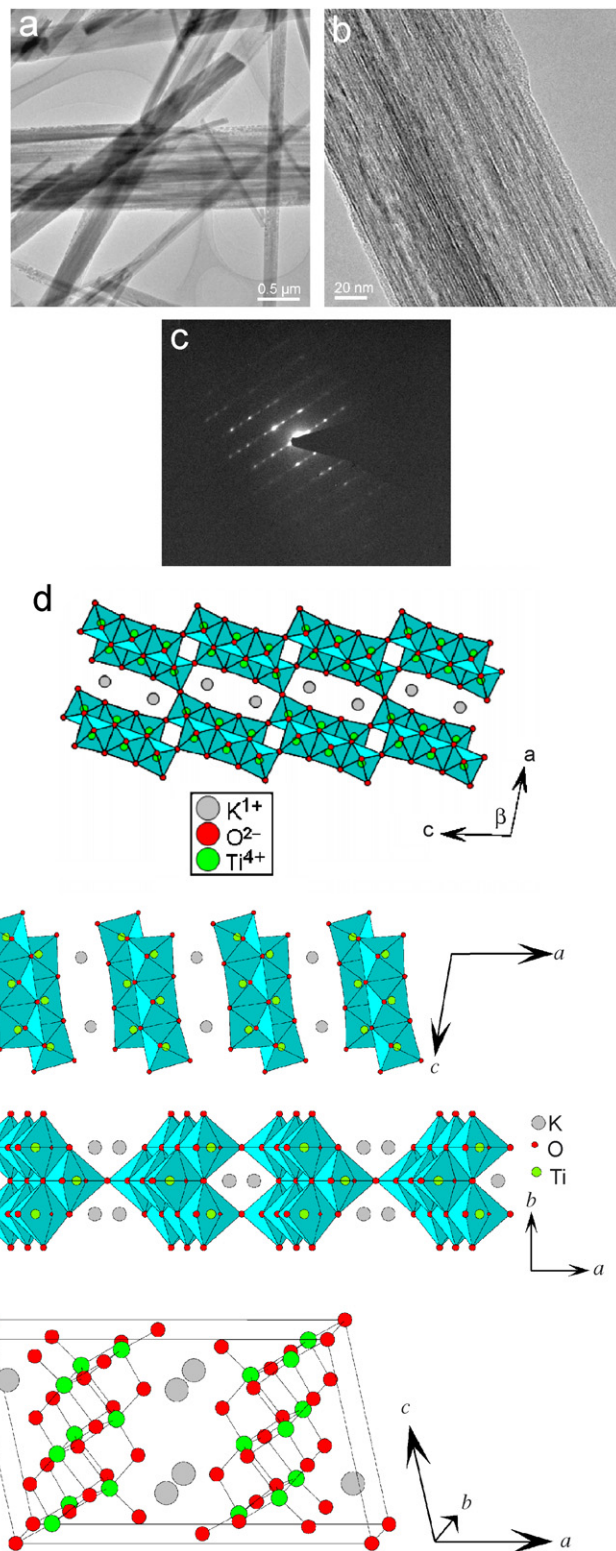


Fig. 8. (a) The low-magnification TEM image of the reaction product taken from concentrated KOH solution; (b) high-resolution TEM image showing a nanowire viewed along [001] exhibiting a well-resolved two-dimensional lattice, the distance between two adjacent layers is ca. 0.78 nm parallel to the nanowire axis; (c) selected area electron diffraction (SAED) patterns of nanowires indicate monoclinic $\text{K}_2\text{Ti}_6\text{O}_{13}$; (d) structural models of $\text{K}_2\text{Ti}_6\text{O}_{13}$; (e) projected along the [010] direction; (f) projected along the [001] direction; and (g) unit cell.

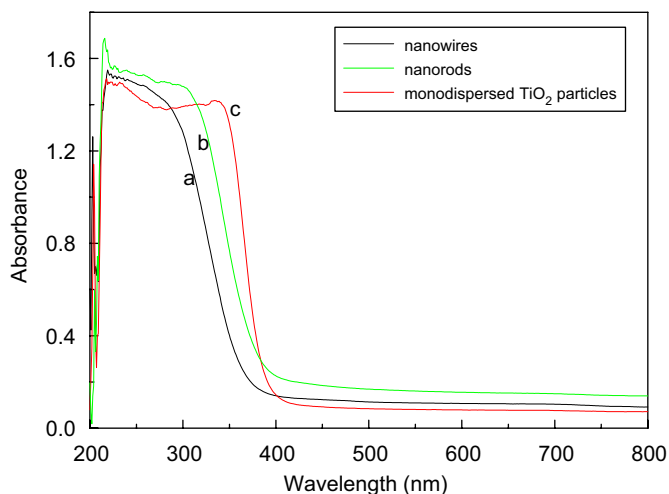


Fig. 9. Experimental UV-visible absorption spectra obtained from (a) nanowires sample, (b) nanorods sample, and (c) monodispersed TiO_2 (anatase) particles sample.

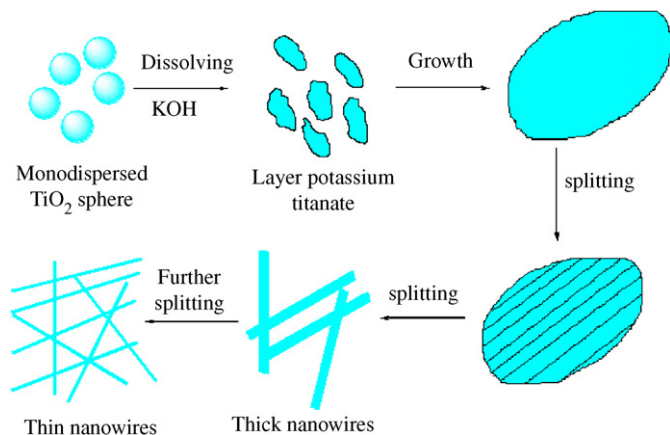


Fig. 10. Schematic drawings depicting the formation process of nanowires.

enhanced in the whole absorption region than that of monodispersed titania sphere.

Schematic drawings depict the formation process of $\text{K}_2\text{Ti}_6\text{O}_{13}$ nanowires as shown in Fig. 10: (a) TiO_2 particles dissolve in the KOH solution and lamellar structures grown on the brim of TiO_2 particles. (b) These lamellar structures grow and adhere along the [001] direction with the (010) plane as the top/bottom surface. Then the potassium titanate lamellar with large area was formed. (c) Splitting of large lamellar structures into nanosheets between (100) and (010) planes occurs. Thick $\text{K}_2\text{Ti}_6\text{O}_{13}$ layers or wires are formed by the splitting of lamellar structures after prolonged reaction. (d) Further splitting of these thick layers or wires between (100) and (010) planes occurs. So the thin $\text{K}_2\text{Ti}_6\text{O}_{13}$ nanowires with large aspect ratio can be obtained by further splitting. It is noticed that the nanowires were obtained by the splitting of layer potassium titanate, so the length of nanowires is determined by the scale of lamellar structures. Monodispersed

TiO_2 submicron sphere is beneficial for the formation and growth of large-area lamellar potassium titanate, and consequently it is in favor of the production of nanowires with a large aspect ratio.

4. Conclusions

In summary, potassium titanate nanowires with a large aspect ratio can be obtained by a simple one-step hydrothermal treatment of monodispersed titania submicron spheres. It is found that the hydrothermal temperature, duration, titanium source and the size distribution of titania raw powder have a great impact on the resultant morphology. Monodispersed raw titania powders are beneficial to obtain long and uniform $\text{K}_2\text{Ti}_6\text{O}_{13}$ nanowires with a large aspect ratio. A formation mechanism is proposed based on the dissolving, growth, thickening and splitting of $\text{K}_2\text{Ti}_6\text{O}_{13}$ nanointermediates. Nanowires with a large aspect ratio may provide the materials basis for the application of solar cell, photocatalysis, and ion change.

Acknowledgments

We gratefully acknowledge the financial support of Program for New Century Excellent Talents in University (Grant no. NCET-05-0278), the National Natural Science Foundation of China (Grant no. 20471012), a Foundation for the Author of National Excellent Doctoral Dissertation of PR China (Grant no. 200322), the Research Fund for the Doctoral Program of Higher Education (Grant no. 20040141004), the Scientific Research Foundation for the Returned Overseas Chinese Scholars, State Education Ministry, and the Younger Teacher Cultivated Foundation of Dalian University of Technology (Grant no. 893230).

References

- [1] Y. Xia, P. Yang, Y. Sun, Y. Wu, B. Mayers, B. Gates, Y. Yin, F. Kim, H. Yan, *Adv. Mater.* 15 (2003) 353.
- [2] (a) P. Hoyer, *Adv. Mater.* 8 (1996) 857;
(b) P. Hoyer, *Langmuir* 12 (1996) 1411.
- [3] (a) Q. Chen, W. Zhou, G. Du, L.M. Peng, *Adv. Mater.* 14 (2002) 1208;
(b) S. Zhang, L.M. Peng, Q. Chen, G.H. Du, G. Dawson, W.Z. Zhou, *Phys. Rev. Lett.* 91 (2003) 256103;
(c) G.H. Du, Q. Chen, R.C. Che, Z.Y. Yuan, L.M. Peng, *Appl. Phys. Lett.* 79 (2001) 3702.
- [4] (a) A.R. Armstrong, G. Armstrong, J. Canales, P.G. Bruce, *Angew. Chem., Int. Ed.* 43 (2004) 2286;
(b) A.R. Armstrong, G. Armstrong, J. Canales, R. Garsia, P.G. Bruce, *Adv. Mater.* 17 (2005) 862;
(c) G. Armstrong, A.R. Armstrong, J. Canales, P.G. Bruce, *Chem. Commun.* 2454 (2005).
- [5] (a) G.K. Mor, K. Shankar, M. Paulose, O.K. Varghese, C.A. Grimes, *Nano Lett.* 6 (2) (2006) 215;
(b) G.K. Mor, O.K. Varghese, M. Paulose, K. Shankar, C.A. Grimes, *Sol. Energy Mater. Sol. Cells* 90 (2006) 2011.
- [6] (a) Z.V. Saponjic, N.M. Dimitrijevic, D.M. Tiede, A.J. Goshe, X. Zuo, L.X. Chen, A.S. Barnard, P. Zapol, L. Curtiss, T. Rajh, *Adv. Mater.* 17 (8) (2005) 965;

- (b) B.M. Rabatic, N.M. Dimitrijevic, R.E. Cook, Z.V. Saponjic, T. Rajh, *Adv. Mater.* 18 (2006) 1033.
- [7] (a) D.V. Bavykin, J.M. Friedrich, A.A. Lapkin, F.C. Walsh, *Chem. Mater.* 18 (2006) 1124;
(b) D.V. Bavykin, V.N. Parmon, A.A. Lapkin, F.C. Walsh, *J. Mater. Chem.* 14 (2004) 3370;
(c) D.V. Bavykin, S.N. Gordeev, A.V. Moskalenko, A.A. Lapkin, F.C. Walsh, *J. Phys. Chem. B* 109 (18) (2005) 8565.
- [8] (a) R. Ma, Y. Bando, T. Sasaki, *Chem. Phys. Lett.* 380 (2003) 577;
(b) R.Z. Ma, T. Sasaki, Y. Bando, *J. Am. Chem. Soc.* 126 (2004) 10382;
(c) R.Z. Ma, K. Fukuda, T. Sasaki, M. Osada, Y. Bando, *J. Phys. Chem. B* 109 (2005) 6210.
- [9] (a) T. Kasuga, M. Hiramatsu, A. Hoson, T. Sekino, K. Niihara, *Langmuir* 14 (1998) 3160;
(b) T. Kasuga, M. Hiramatsu, A. Hoson, T. Sekino, K. Niihara, *Adv. Mater.* 11 (1999) 1307.
- [10] (a) H.Y. Zhu, Y. Lan, X.P. Gao, S.P. Ringer, Z.F. Zheng, D.Y. Song, J.C. Zhao, *J. Am. Chem. Soc.* 127 (2005) 6730;
(b) H.Y. Zhu, X.P. Gao, Y. Lan, D.Y. Song, Y.X. Xi, J.C. Zhao, *J. Am. Chem. Soc.* 126 (2004) 8380;
(c) Y. Lan, X.P. Gao, H.Y. Zhu, Z.F. Zheng, T.Y. Yan, F. Wu, S.P. Ringer, D.Y. Song, *Adv. Funct. Mater.* 15 (8) (2005) 1310.
- [11] X. Sun, Y. Li, *Chem. Eur. J.* 9 (2003) 2229.
- [12] (a) D. Wu, J. Liu, X.N. Zhao, A.D. Li, Y.F. Chen, N.B. Ming, *Chem. Mater.* 18 (2006) 547;
(b) D. Wu, Y.F. Chen, J. Liu, X.N. Zhao, A.D. Li, N.B. Ming, *Appl. Phys. Lett.* 87 (11) (2005) 112501.
- [13] C.Y. Xu, Q. Zhang, H. Zhang, L. Zhen, J. Tang, L.C. Qin, *J. Am. Chem. Soc.* 127 (2005) 11584.
- [14] Y.B. Mao, S.S. Wong, *J. Am. Chem. Soc.* 128 (2006) 8217.
- [15] B.X. Wang, X.P. Zhao, *Adv. Funct. Mater.* 15 (11) (2005) 1815.
- [16] J.B. Yin, X.P. Zhao, *Nanotechnology* 17 (1) (2006) 192.
- [17] (a) C.C. Tsai, H. Teng, *Chem. Mater.* 16 (2004) 4352;
(b) C.C. Tsai, H. Teng, *Chem. Mater.* 18 (2006) 367;
(c) J.N. Nian, H. Teng, *J. Phys. Chem. B* 110 (2006) 4193.
- [18] L. Qian, F. Teng, Z.S. Jin, Z.J. Zhang, T. Zhang, Y.B. Hou, S.Y. Yang, X.R. Xu, *J. Phys. Chem. B* 108 (2004) 13928.
- [19] (a) Y. Wang, H. Xu, X. Wang, X. Zhang, H. Jia, L. Zhang, J. Qiu, *J. Phys. Chem. B* 110 (2006) 13835;
(b) X.C. Jiang, T. Herricks, Y.N. Xia, *Adv. Mater.* 15 (14) (2003) 1205;
(c) S. Eiden-Assmann, J. Widoniak, G. Maret, *Chem. Mater.* 16 (2004) 6.
- [20] Y.C. Zhu, H.L. Li, Y. Koltypin, Y.R. Hachohen, A. Gedanken, *Chem. Commun.* (2001) 2616.
- [21] (a) J. Yang, Z. Jin, X. Wang, W. Li, J. Zhang, S. Zhang, X. Gao, Z. Zhang, *Dalton Trans.* (2003) 3898;
(b) Y.Q. Wang, G.Q. Hu, X.F. Duan, H.L. Sun, Q.K. Xue, *Chem. Phys. Lett.* 365 (2002) 427.
- [22] (a) Z.Y. Yuan, X.B. Zhang, B.L. Su, *Appl. Phys. A* (2003);
(b) Z.Y. Yuan, B.L. Su, *Colloids Surf. A* 241 (2004) 173.
- [23] (a) B.L. Wang, Q. Chen, R.H. Wang, L.M. Peng, *Chem. Phys. Lett.* 376 (2003) 726;
(b) R.H. Wang, Q. Chen, B.L. Wang, S. Zhang, L.M. Peng, *Appl. Phys. Lett.* 86 (2005) 133101;
(c) G.H. Du, Q. Chen, P.D. Han, Y. Yu, L.M. Peng, *Phys. Rev. B* 67 (2003) 035323.